



PERGAMON

Acta mater. Vol. 47, No. 8, pp. 2567–2579, 1999
© 1999 Acta Metallurgica Inc.
Published by Elsevier Science Ltd. All rights reserved
Printed in Great Britain
1359-6454/99 \$20.00 + 0.00

PII: S1359-6454(99)00059-2

SYNTHESIS AND CHARACTERIZATION OF MECHANICALLY ALLOYED AND SHOCK-CONSOLIDATED NANOCRYSTALLINE NiAl INTERMETALLIC

T. CHEN, J.M. HAMPIKIAN† and N.N. THADHANI

School of Materials Science and Engineering, Georgia Institute of Technology, 778 Atlantic Drive, Atlanta, GA 30332-0245, U.S.A.

(Received 28 April 1998; accepted in revised form 4 February 1999)

Abstract—The synthesis, microstructural characterization and microhardness of nanocrystalline B2-phase NiAl intermetallic are discussed in this paper. Nanophase NiAl powders were prepared by mechanical alloying of elemental Ni and Al powders under an argon atmosphere for different times (0–48 h). The alloyed nanocrystalline powders were then consolidated by shock compaction at a peak pressure of 4–6 GPa, to 83% dense compacts. Characterization by transmission electron microscopy (TEM) revealed that the microstructure of the shock-consolidated sample was retained at the nanoscale. The average crystallite size measurements revealed that mechanically alloyed NiAl grain size decreased from 48 ± 27 to 9 ± 3 nm with increasing mechanical alloying time from 8 to 48 h. The long-range-order parameters of powders mechanically alloyed for different times were determined, and were observed to vary between 0.82 for 5 h and 0.63 for 48 h of milling time. Following shock compaction, the long-range-order parameter was determined to be 0.76, 0.69 and 0.66, respectively, for the 16, 24 and 48 h alloyed specimens. Both the mechanically alloyed nanocrystalline NiAl powder and the shock-consolidated bulk specimen showed evidence of grain boundary dislocations, subgrains, and distorted regions. A large number of grain boundaries and defects were observed via high resolution TEM (HRTEM). Shear bands were also observed in the mechanically alloyed NiAl intermetallic powders and in the shock-consolidated compacts. Microhardness measurements of shock-consolidated material showed increasing microhardness with increasing crystallite size refinement, following Hall–Petch behavior. © 1999 Acta Metallurgica Inc. Published by Elsevier Science Ltd. All rights reserved.

Keywords: Powder consolidation, dynamic compaction; Mechanical alloying; Hardness; Shear bands

1. INTRODUCTION

Nanocrystalline materials, defined as polycrystalline solids having crystallite sizes usually less than 100 nm, can exhibit unique properties due to the large fraction of grain boundaries that they possess. In particular, the strength, ductility, and diffusion kinetics, among other mechanical and chemical properties, may be significantly enhanced for nanocrystalline materials in comparison with materials with conventional grain sizes [1–4].

In the nickel–aluminum alloy system, equiatomic NiAl (B2-phase) exhibits a high melting temperature (1640°C), a low density (5.9 g/cm^3 , which is approximately $2/3$ that of Ni based superalloys), metal-like electrical and thermal conductivity, and a lower DBTT relative to other intermetallics. NiAl has potential applications such as in hot sections of gas turbine engines for aircraft-propulsion systems, bond coats under thermal barrier coatings, electronic metallization compounds in advanced semi-

conductor heterostructures, and surface catalysts [5]. Most research efforts on improving the ductility of NiAl have been focused on the addition of metalloids (e.g. B) to pin the grain size.

The synthesis of nanocrystalline alloys and intermetallic compounds by ball milling has been successfully achieved by several researchers [6–10]. In the case of nanocrystalline NiAl alloy powders, subsequent consolidation has been accomplished by means of hot pressing [10], vacuum hot pressing [10], and extruding [11] at elevated temperatures (1275–1473 K). Long-term temperature excursions associated with these processes can allow primary recrystallization and grain growth. Smith has reported sinter-forging of mechanically alloyed nanocrystalline NiAl alloy [8], with a retained grain size of 72 ± 41 nm.

Shock-wave compaction has been employed for consolidation of powders of nanocrystalline alloys [1, 12], as well as metastable (amorphous) compounds [13, 14]. The application of a shock-wave produces a high pressure of microsecond duration and temperatures moderate enough to attain

†To whom all correspondence should be addressed.

bonding between powders, resulting in compacted samples with high density and retained parent structure [15]. In this study, nanocrystalline NiAl alloy powders were first obtained by ball milling elemental Ni and Al powders, which were subsequently shock-consolidated to produce dense compacts for microstructural characterization and hardness measurements.

2. EXPERIMENTAL

Ni and Al powders of nominal purity of 99.9% and 99.97%, and particle sizes ranging between 45–150 μm and 45–75 μm , respectively, were mixed at a 1:1 mole ratio and sealed in a plastic bottle, which was placed in a V-blender for blending the powders for 24 h. For mechanical alloying, approximately 5 g of powder, with two steel balls (ball-to-powder weight ratio of approximately 3.3 to 1), were put into the AISI 304 stainless steel milling vial. The milling was performed in a Spex 8000 laboratory ball mill for time periods ranging between 0 and 48 h at room temperature. It was found that the 5 h run was sufficient for the Ni and Al to alloy and form intermetallic NiAl. Powders alloyed for 16, 24 and 48 h were used for compaction experiments. At all times the powders were handled and sealed in containers in a glove box under argon atmosphere in order to minimize exposure to the ambient.

Shockwave compaction was accomplished with a three-capsule, plate impact fixture, using the Georgia Tech 80 mm diameter single-stage gas gun. Details of the fixture and gun loading technique are described elsewhere [16]. The powders were packed in capsules, prior to shock consolidation, at about 70% of theoretical maximum density. Impact experiments were performed using an aluminum projectile and a 5 mm thick stainless steel flyer plate accelerated in the 80 mm diameter gas gun, at an impact velocity measured to be approximately 400 m/s. Peak pressures corresponding to these loading conditions were computed using a two-dimensional AUTODYNE-2D hydrodynamic code [16]. The hydrodynamic properties of a mechanical mixture of Ni and Al were considered for the simulation. Following an initial pressure wave of 1 GPa, a bulk peak pressure of 4–6 GPa was predicted due to two-dimensional radial wave-focusing effects. Since two-dimensional wave-focusing effects dominate the loading conditions, the peak pressures generated are independent of material properties. The samples were recovered in the form of 10 mm diameter by 3 mm thick discs. The density of the samples following shock compaction was determined by the Archimedes method.

X-ray diffraction analysis was performed with a Philips X-1800 diffractometer in step scanning mode using Ni-filtered $\text{CuK}\alpha$ radiation to determine the crystal structure and crystallite size. Scanning electron microscopy (SEM) was carried out with a

Hitachi S-800 field emission scanning electron microscope to characterize the milled powder morphology and the compact surfaces. Transmission electron microscopy (TEM) characterization utilized using a 200 kV field emission transmission electron microscope. TEM samples were prepared by ultrasonically dispersing the mechanically alloyed NiAl powder in ethanol and then placing one drop onto a holey carbon support grid. The shock-consolidated samples were cut longitudinally along the direction of shock-wave propagation, for characterization of the cross-section and for preparing TEM samples which were made using an ion polishing system at low incident angle (Gatan PIPS).

Shock-consolidated samples were tested for Vickers microhardness using a Leco DM-400F Hardness Tester. The indentations were made in regions of the specimens that appeared to have nearly full density.

The crystallite sizes of both mechanically alloyed powder and shock-compacted bulk NiAl specimen were measured by the ASTM linear intercept method on the bright and dark field TEM micrographs, which yields an area-weighted average grain size.

3. RESULTS

In this work nanocrystalline NiAl intermetallic alloy powders were prepared by mechanical alloying elemental powders for a period of 0–6 h (at 1 h intervals) 8, 16, 24 and 48 h. The 16, 24 and 48 h ball-milled powders were subsequently shock-consolidated to obtain bulk compacts, at a peak pressure of approximately 4–6 GPa using a gas gun system for impact loading.

3.1. Mechanical alloying of nanocrystalline NiAl intermetallic alloy

The synthesis of nanocrystalline NiAl alloy, by ball milling (from 0–48 h) elemental Ni and Al powders mixed in a 1:1 atom ratio, was confirmed by X-ray diffraction analysis. As shown in the XRD traces in Fig. 1(a), almost complete alloying is achieved beyond 5 h of milling time. The degree of order of the NiAl powder was calculated from the square root of the intensity ratio of the superlattice reflection (100) to the fundamental reflection (110), by normalizing this ratio to the calculated intensity ratio for completely ordered NiAl [17]. The variation of long-range-order parameter (S) for the mechanically alloyed NiAl, as a function of milling time is shown in Fig. 1(b).

The morphology of alloyed powders produced at different alloying times was investigated via SEM analysis. As shown in Figs 2(a)–(f), the early stages of mechanical alloying (2 h and 5 h) result in the formation of powder agglomerates having a wide range in size (from 5 μm to 430 μm). The particles agglomerate as a result of the repeated welding

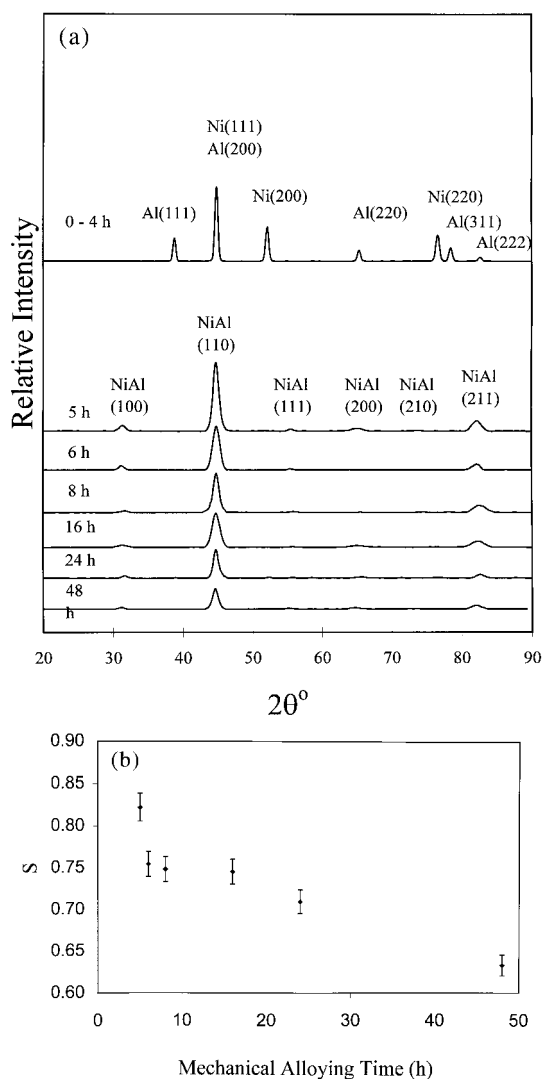


Fig. 1. (a) X-ray diffraction patterns of ball-milled NiAl powders showing the progress of mechanical alloying as a function of milling time; (b) plot of long-range-order parameter of mechanically alloyed NiAl alloy powders as a function of alloying time.

during milling. Further milling leads to increased deformation and work hardening, and the agglomerated powders then disintegrate into fragments producing finer particles of approximately $0.7 \pm 0.3 \mu\text{m}$ in size [Figs 2(c)–(f)]. The particles shown in Figs 2(c)–(f) consist of nanosized crystallites.

The nanocrystalline structure of the powders was confirmed by TEM imaging, as shown in the dark field images in Figs 3(a)–(d). The representative electron diffraction pattern shown in Figs 3(a)–(d) confirms that NiAl was the only crystalline phase detected in the mechanically alloyed powders that received more than 5 h of ball milling. The size of the diffraction crystallites determined from TEM images of the ball-milled particles shows that the grain size decreases from approximately 50 nm to

Table 1. Contamination of Fe for NiAl alloyed for different times

Mechanical alloying time (h)	Fe (at.%)
8	0.35
16	0.22
24	0.84
48	3.21

10 nm with increasing milling time from 8 h to 48 h. The variation in average grain size (obtained from TEM micrographs) plotted as a function of alloying time is shown in Fig. 4.

Some iron contamination of the powders was observed by TEM analysis using EDS. The variation of Fe impurity concentration, determined via quantitative EDS analysis, was found to be approximately 0.8 at.% after 8 h milling, and increased to approximately 3.2 at.% with 48 h of mechanical alloying time, as shown in Table 1.

High resolution TEM (HRTEM) imaging of the mechanically alloyed powders was used to characterize the substructure of the crystallites. During the process of ball milling, large deformation is introduced, which can produce distorted regions, within subgrains, grain boundaries, and even across entire grains. The distorted regions are generated by an accumulation of dislocations from other regions. This sort of distortion is not commonly observed in coarse-grained materials. HRTEM imaging of the mechanically alloyed powders (milled for 24 h) revealed the presence of moiré fringes, stacking faults and distorted grains, as shown in Fig. 5(a). Figure 5(b), an enlarged image of region A in Fig. 5(a), shows the deformation substructure in the grains more clearly. Edge dislocations were also identified in the HRTEM images [circled in Fig. 5(b)], indicated by the presence of an extra half plane. The bands shown in the grains in Fig. 5(b), as well as in the grains in Fig. 5(a), have also been observed in other studies [18], and have been identified as shear bands. It has been reported that the formation of these shear bands is responsible for breakdown of the grains and generation of nanostructure during mechanical alloying.

3.2. Shock consolidation of mechanically alloyed nanocrystalline NiAl powders

Shock compaction of the mechanically alloyed nanocrystalline NiAl powders, performed at an impact velocity of 400 m/s (4–6 GPa peak pressure), produced single piece discs approximately 10 mm in diameter and 3 mm in thickness. The shock-densified NiAl powder compacts had both micro- and macro-cracks propagating radially outward from the compact axis, and were clearly observed from optical microscopy. The radial cracks in the compacts are produced due to two-dimensional radial wave-focusing effects. The densities of the shock-compacted NiAl powders mechanically alloyed for 16, 24 and 48 h were measured to be 4.81–4.88 g/

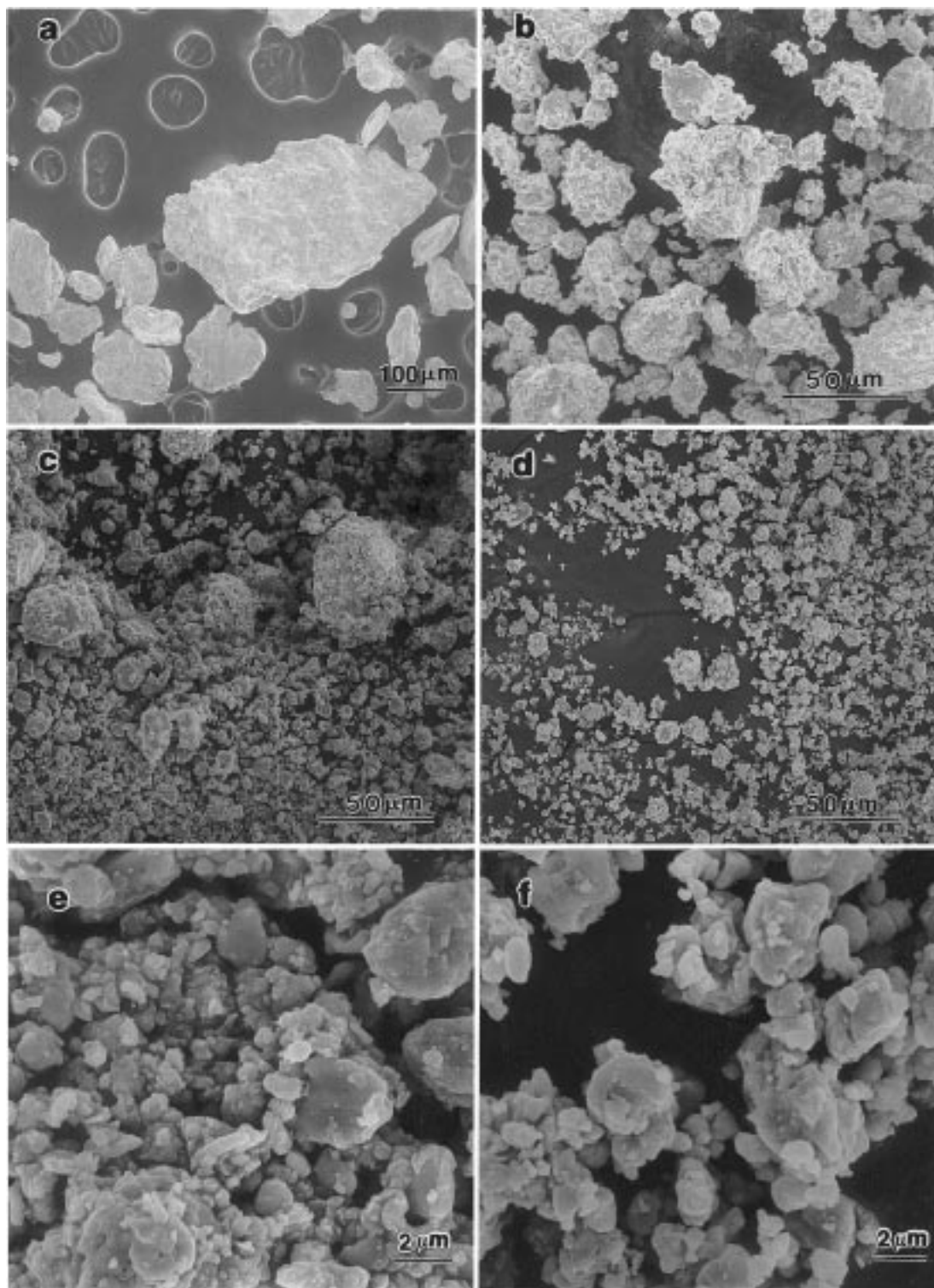


Fig. 2. Morphology of Ni–Al powders milled for (a) 2 h, (b) 5 h, (c) 8 h, (d) 16 h, (e) 24 h, and (f) 48 h.

cm^3 , which is approximately 83% of the theoretical maximum density of B2–NiAl, as shown in Table 2. Since nanocrystalline NiAl possesses a larger volume fraction of grain boundaries than conventional NiAl, its theoretical solid density value may be lower, and thus the relative density of the shock-

consolidated compacts may be somewhat higher. It should also be noted that the shock-consolidation conditions employed in this work were by no means optimized.

The X-ray diffraction patterns of the shock-consolidated compacts of powders alloyed for 16, 24

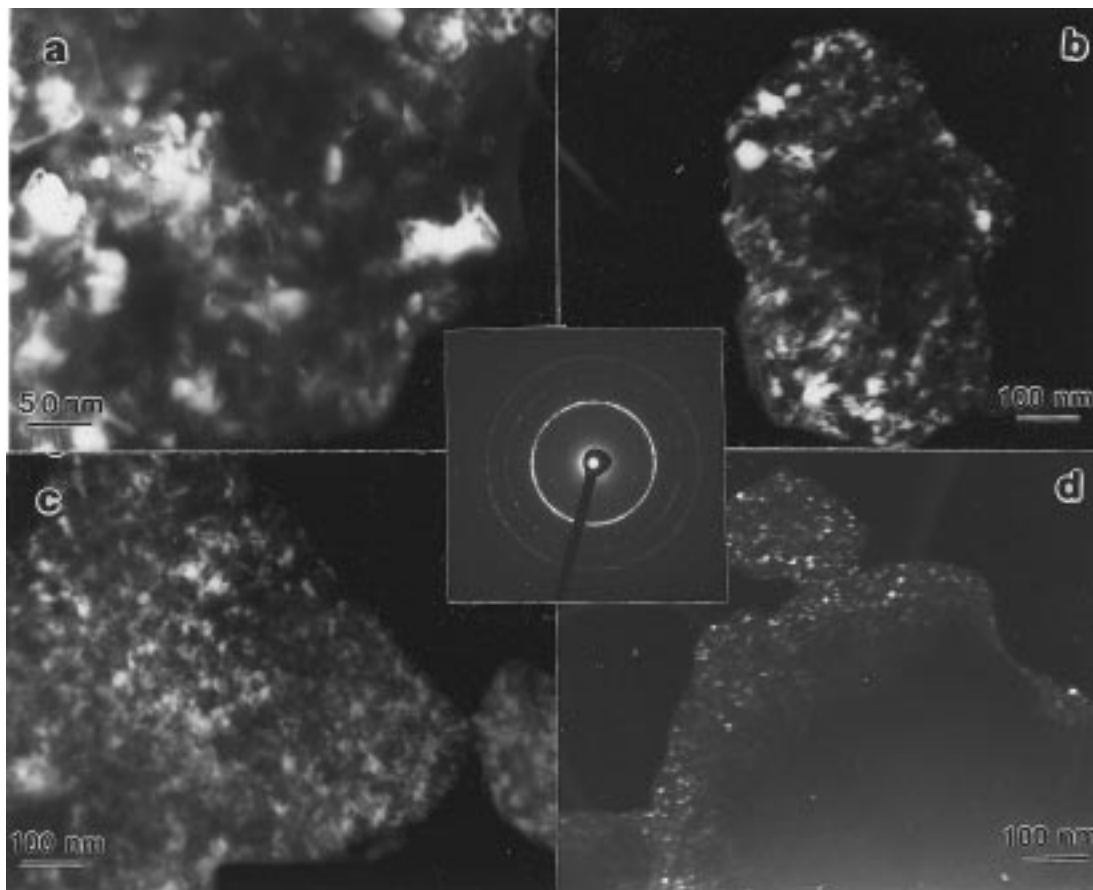


Fig. 3. Dark field images of nanocrystalline NiAl particles ball-milled for (a) 8 h, (b) 16 h, (c) 24 h, (d) 48 h and a typical electron diffraction pattern.

Table 2. Density of shock-compacted NiAl

Mechanical alloying time (h)	Measured density (g/cm^3)	Relative density (%)
16	4.88	83
24	4.87	83
48	4.81	82

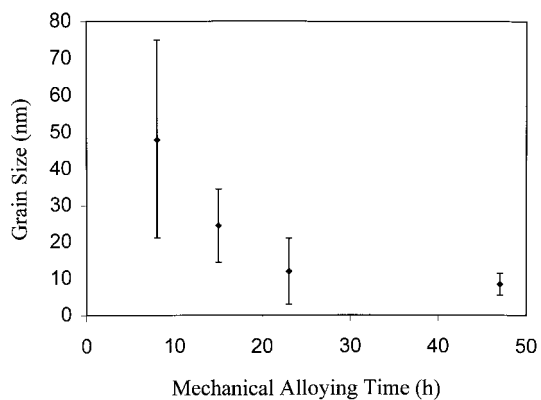


Fig. 4. Plot of average grain size varying as a function of mechanical alloying time.

and 48 h are shown in Fig. 6(a). It can be seen that the nanocrystalline NiAl phase of the mechanically alloyed powder was retained after shock compaction. The broadened diffraction patterns are attributed to the effects of the nanoscale crystallite size and retained residual stress. The long-range-order parameter (S), calculated from these shock-densified samples and plotted as a function of milling time, is shown in Fig. 6(b). The degree of order for the shock-compacted samples is observed to remain practically unchanged relative to the mechanically alloyed powders shown in Fig. 1(b). However, for the hot pressing consolidation method employed by Pyo *et al.* [10] the degree of order was observed to increase, as compared to the mechanically alloyed sample, from 0.56 to 0.77. This has been explained as being due to the homogenization effect of hot pressing on the composition, in addition to the annealing of the defects.

An SEM micrograph of a cross-section of the shock-compacted sample, shown in Fig. 7(a), reveals the presence of voids, indicating that under the consolidation conditions used, complete densification is not achieved. The SEM micrograph of the fracture surface of the shock-compacted sample, shown in Fig. 7(b), reveals that the fracture occurs

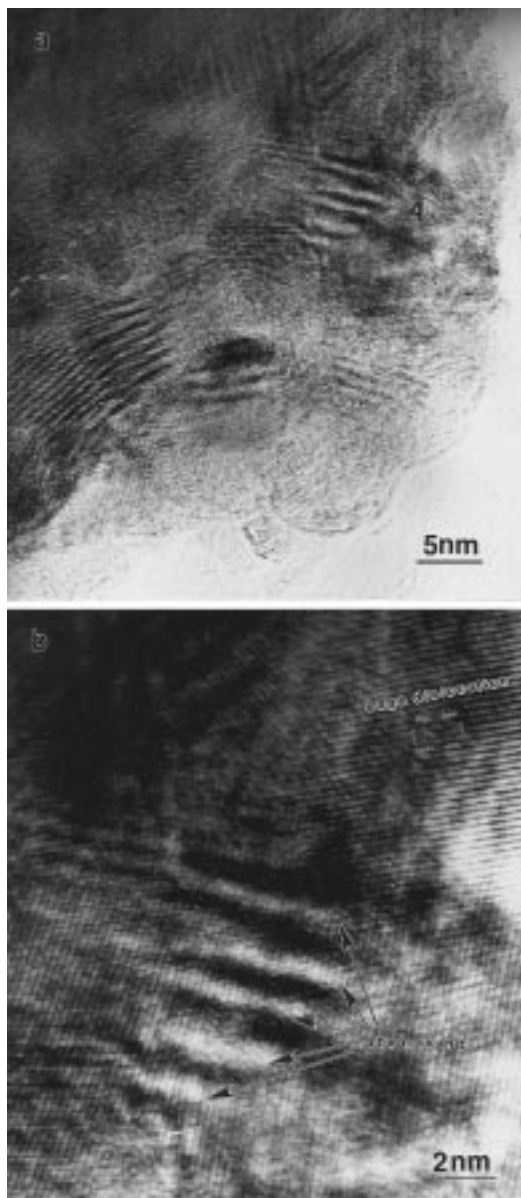


Fig. 5. High resolution images of mechanically alloyed (milled for 24 h) nanocrystalline NiAl particles: (a) grains are marked using dashed lines; (b) an enlarged image of region A from (a). Edge dislocation is marked.

along inter-particle boundary regions, leaving particles intact, confirming the lack of complete metallurgical bonding.

TEM analysis of shock-densified compacts of 16, 24 and 48 h alloyed powders, shown in Figs 8(a)–(c), reveals a distribution of diffracting crystallites, which is consistent with a reduction in size observed with mechanically alloyed powders as a function of milling time. Average grain sizes range from 27 ± 18 nm at 16 h ball milling to 9 ± 6 nm at 48 h ball milling. The representative electron diffraction pattern shown in the Fig. 8(d) confirms that the only phase present is crystalline B2-phase nickel–aluminide, in agreement with X-ray diffraction

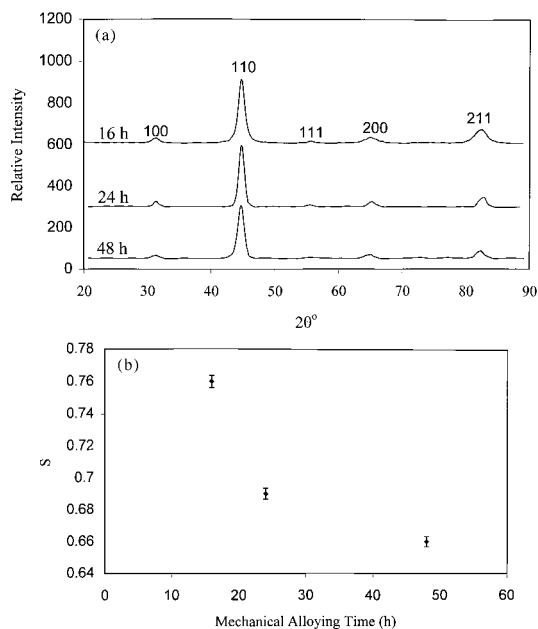


Fig. 6. (a) X-ray diffraction pattern of shock-consolidated NiAl; (b) plot of long-range parameter of shock-compacted NiAl alloy as a function of mechanical alloying time.

results. The TEM results, therefore, demonstrate that the nanocrystalline B2–NiAl microstructure is maintained in the shock-consolidated compacts.

HRTEM images shown in Figs 9(a) and (b), taken from the shock-consolidated NiAl (alloyed for 24 h), illustrate presence of moiré fringes, distorted grain regions, and shear bands in the interior of the grains, similar to that observed in the mechanically alloyed powders. Shear bands spanning across several grain dimensions are also observed as shown in Fig. 9(b). High magnification bright field TEM imaging in Figs 10(a)–(c) further revealed interesting deformation and shear band patterns. The shear bands in Fig. 10(a) are approximately 15 nm in thickness and those in Fig. 10(b) are approximately 100 nm thick. A multitude of even finer grains appears to be formed inside these shear band region, supporting the hypothesis that shear bands provide the mechanism for grain size refinement [18]. The TEM micrographs of the shock-consolidated specimen, shown in Figs 10(a) and (b), indicate preferred orientation of grains along the direction of band formation. The shear bands also include grains showing lattice rotation and flow. The shear bands in the shocked samples span several grain dimensions and are 100–500 nm long in contrast to those observed in the powders, which were 12 nm in length and confined to a single grain. Selected area diffraction patterns (SADP) taken from bands A and B, in Fig. 10(b), show the diffraction spots to be highly streaked indicating extensively strained crystallites. The formation of shear bands in the shock-densified compacts is con-

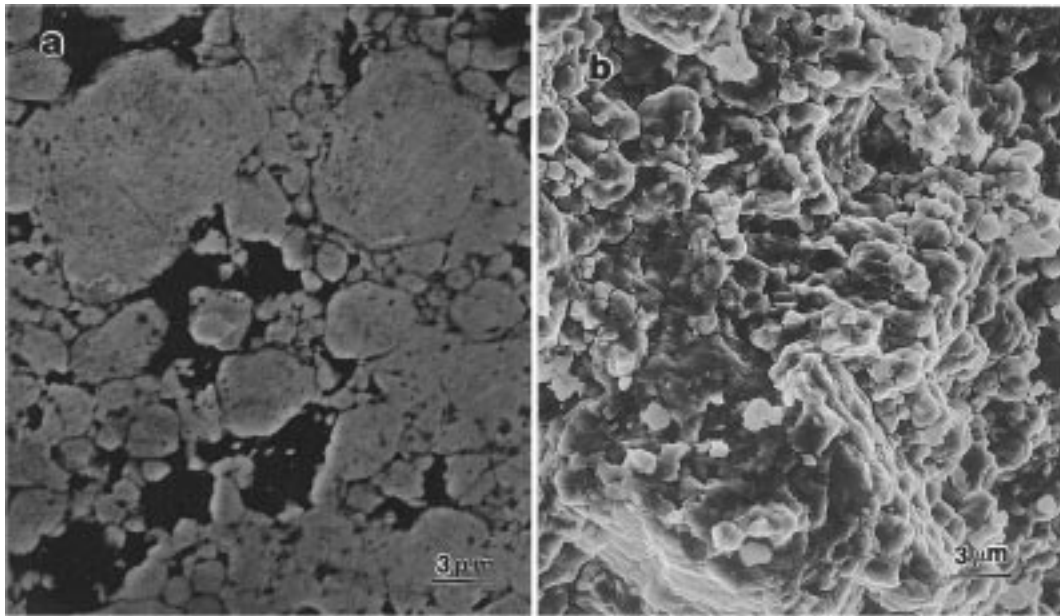


Fig. 7. SEM micrographs of shock-consolidated nanocrystalline NiAl: (a) cross-section, (b) fracture surface.

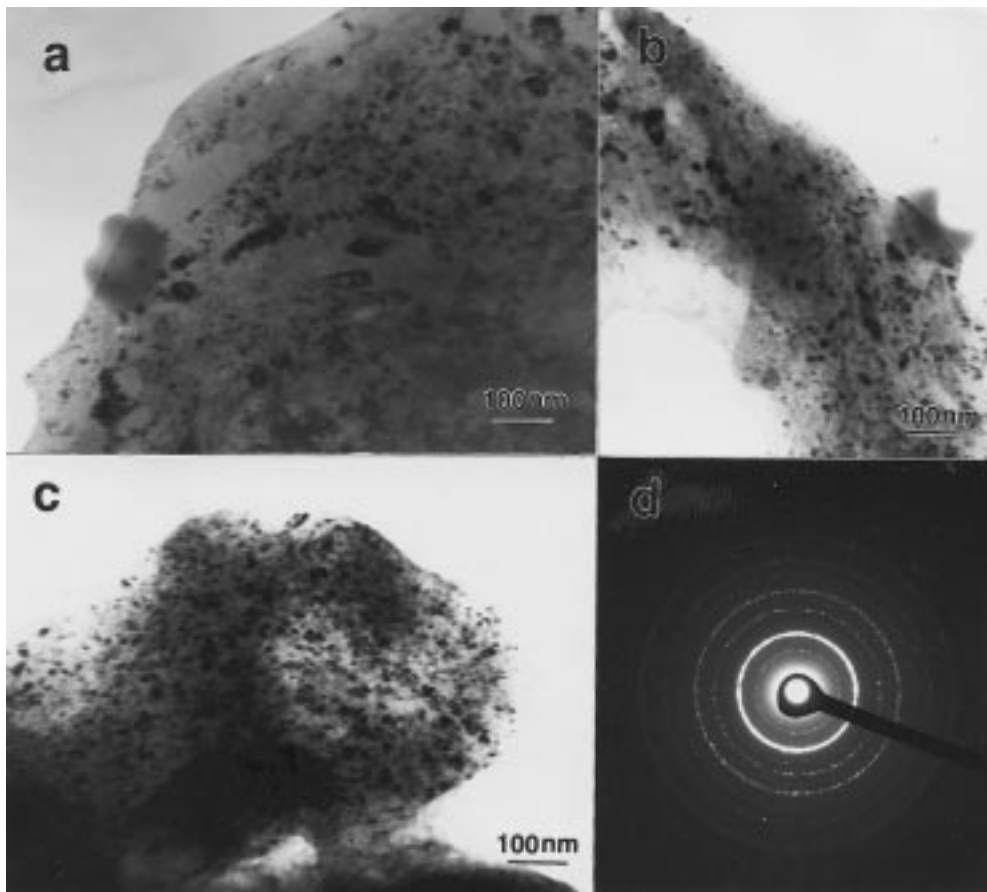


Fig. 8. TEM bright field images of shock-densified NiAl intermetallic compacts of (a) 16 h, (b) 24 h, (c) 48 h alloyed powders, and (d) a typical electron diffraction pattern.

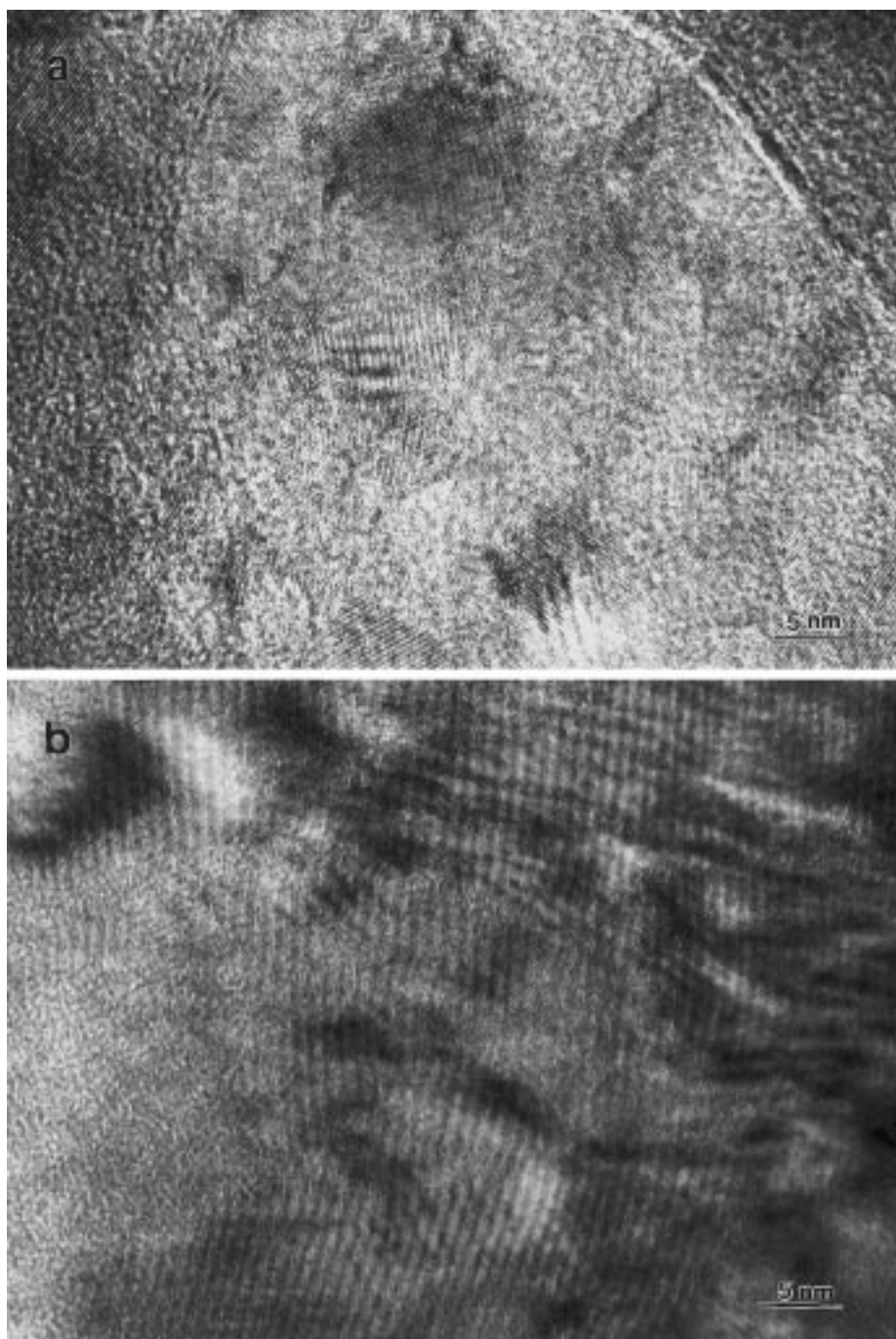


Fig. 9. HRTEM images of shock-consolidated NiAl compacts (alloyed for 24 h): (a) moiré fringes, distorted regions, and shear bands in the interior of grains are identified; (b) shear bands span several grain dimensions.

sidered to be induced by non-homogeneous deformation at high strain rate [19].

The results of Vickers microhardness measurements performed on metallurgically polished consolidated specimens are shown in Fig. 11. It is observed that the microhardness increases with increasing grain size refinement, from approximately 650 to 800 HV as average grain size changed

from 27 ± 18 nm (with 16 h ball milling) to 9 ± 6 nm (with 48 h ball milling). These measured microhardness values are much higher than the hardness of coarse-grained polycrystalline NiAl (330 HV reported by Haubold *et al.* [20]). Cracking was not observed around the indentations, which suggests that significant plastic deformation can be accommodated. This is similar to the results

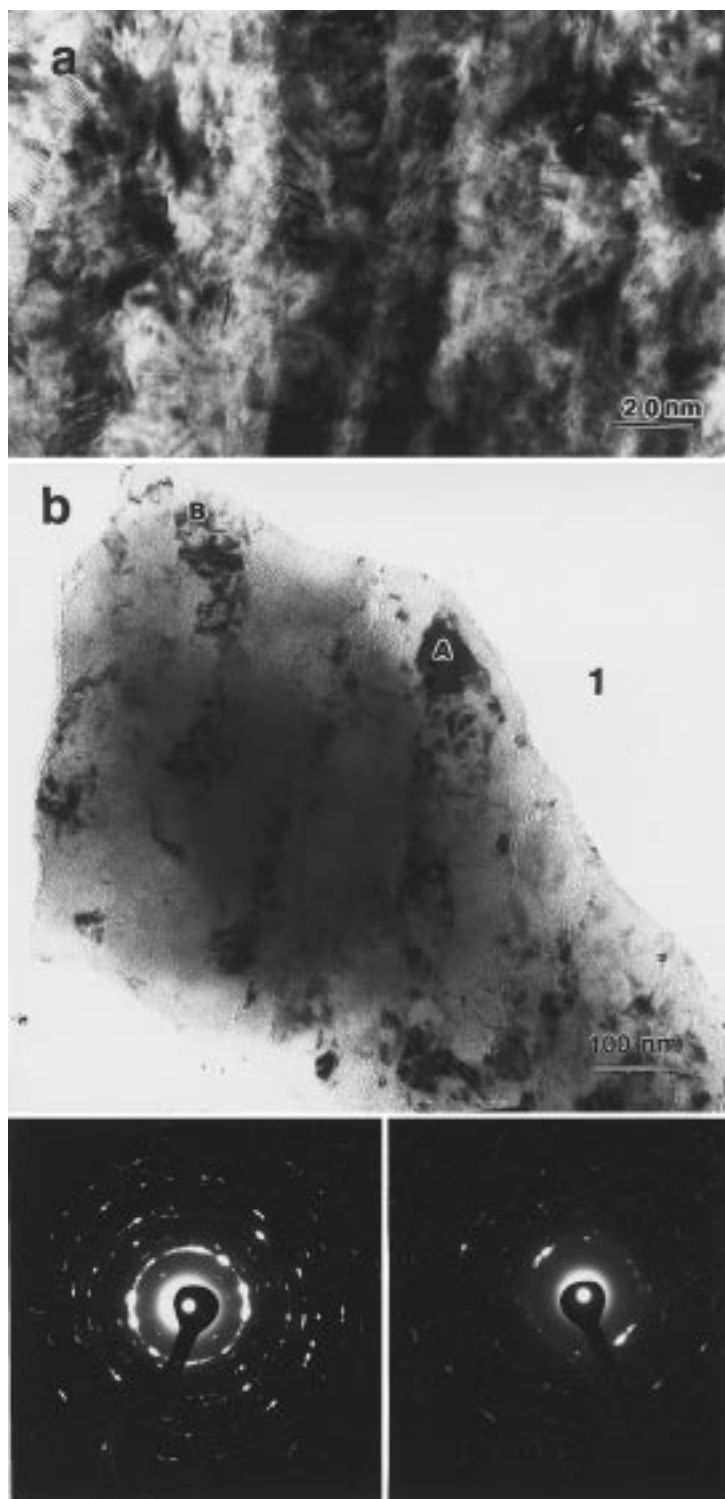


Fig. 10. TEM micrographs of interesting deformation and shear band patterns: (a) shear bands are about 15 nm in thickness; (b) shear bands are about 100 nm thick. SADPs from region A and B indicate extensively strained crystallites.

observed by Jain *et al.* [21] on nanocrystalline titanium–aluminide. The Vickers microhardness of nanocrystalline NiAl compacts has been measured to be in the range of 460–480 HV for sinter-forged

NiAl [8], 603 HV for vacuum hot-pressed NiAl and 564 HV for hot-pressed NiAl [10], 550–575 HV for NiAl with grain size of 0.5 μm . The differences in the hardness values are associated with differences

in retained porosity as well as actual crystallite size. Haubold *et al.* [20] observed that 78% dense NiAl compacts prepared via inert gas condensation and subsequent compaction at 1 GPa showed a hardness of 540 HV. However, annealing of the porous compacts at 750°C for 5 h increased the density to 80% TMD and correspondingly the hardness changed to 723 HV. Further hot pressing (at 450°C) increased the hardness to 887 HV. Smith found 650–697 HV for mechanically milled and double-forged NiAl (grain size about 72 ± 41 nm, 94% dense) [32, 33].

4. DISCUSSION

4.1. Synthesis of nanocrystalline B2-phase NiAl intermetallic

Mechanical alloying is a high energy operation involving repeated welding, fracturing, and rewelding of powder particles. During mechanical alloying of NiAl, the powders agglomerate first, then disintegrate and reweld together at a fine scale. The repetitive welding and fracturing of the powders is a common mechanism for mechanical alloying of powders. In the case of a highly exothermic powder mixture, an abrupt self-sustained reaction can also occur resulting in alloy formation. The XRD patterns of the mechanically alloyed powders, shown in Fig. 1(a), indicate that synthesis of NiAl from elemental Ni and Al powders takes place by a solid state reaction. These results reveal a very abrupt reaction with no alloying up to 4 h of milling and complete alloying in 5 h. Increasing milling time results in further reduction of average crystallite size and microstrain storage, which is in agreement with early studies on mechanical alloying of NiAl. The synthesis of nanoscale crystallites of NiAl by mechanically alloying using ball milling has also been shown by other researchers [8, 9]. Atzmon demonstrated that NiAl is produced via ball milling as a result of an explosive, exothermic reaction, driven by a large heat of compound formation (–59 to –72 kJ/mol), instead of a gradual solid state layer diffusion [9]. With continued milling of the alloyed powders, the formation of shear bands results in regions of extensive deformation in which grains undergo further reduction in size and ultimately

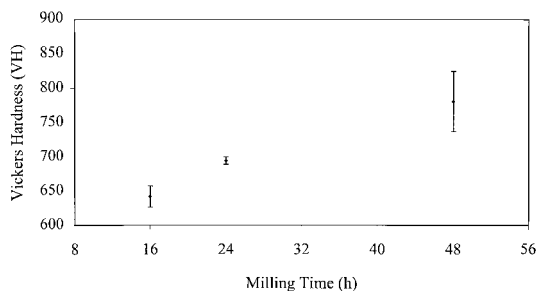


Fig. 11. Microhardness of shock-consolidated NiAl.

produce a nanocrystalline structure with extensive disorder.

Disordering by mechanical alloying is a common phenomenon for b.c.c. compounds. The degree of ordering obtained in mechanically alloyed intermetallics is a balance between disordering from the mechanical alloying process and thermally activated reordering. The ordering energy (ΔH) of an intermetallic compound can be approximately predicted from the enthalpies of formation by the Bragg–Williams theory [23] under the assumption of homogeneous disordering, and ignoring entropy effects.

$$\Delta H = \frac{1}{2} \varepsilon H_f S^2. \quad (1)$$

In this equation, ε is the pair exchange energy, which equals unity in this case, H_f is the formation energy, and S is the long-range-ordering parameter. The enthalpy of formation for NiAl has been reported to be approximately –59 kJ/mol, and recent studies report a value near –72 kJ/mol [5]. Compared to non-stoichiometric Ni–Al alloys, stoichiometric Ni–Al has the lowest formation enthalpy as shown by Fig. 12 [5, 24–27], which leads to the conclusion that stoichiometric NiAl has the greatest tendency to reorder, and that complete disordering of the B2 NiAl is energetically unfavorable. This may explain the finding that NiAl did not amorphize under the mechanical alloying conditions used in the present work, but did change to a metastable partially disordered state accompanied by a reduction in particle and crystallite sizes and microstrain storage. The enthalpy change associated with the reduction of the ordering parameter from 1 to 0.63 (milled for 48 h) is calculated to be –26.6 kJ/mol, using $H_f = -72$ kJ/mol. The final state of mechanically alloyed NiAl will be a dynamic equilibrium between thermal reordering from the stored enthalpy and mechanical disordering introduced during ball milling.

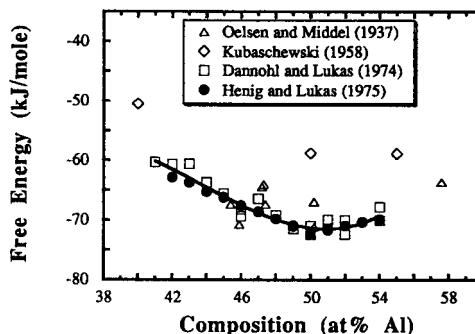


Fig. 12. The free energy of formation of NiAl as a function of composition [5]. Reprinted from *Acta Metallurgica et Materialia*, Volume 43, D. B. Miracle, “The physical and mechanical properties of NiAl”, pp. 649–684, 1993, with permission from Elsevier Science Ltd.

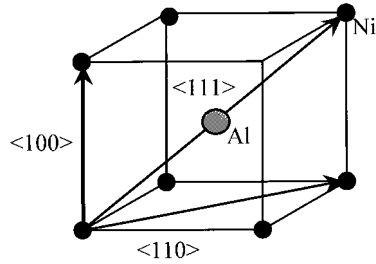


Fig. 13. B2 crystal structure.

The disorder generated by continued ball milling of Ni–Al alloy powders is a complex process, which involves destruction of chemical order, reduction of crystallite size, and an increase of lattice strain and defects. Aluminides with the B2 ordered structure (Fig. 13) can accommodate very high concentrations of vacancies in their lattice. In the present work, a large number of grain boundaries, distorted subgrains, distorted grain boundaries, grain boundary dislocations, and shear bands, in addition to Fe impurities, were detected in the mechanically alloyed powders.

The adiabatic temperature rise produced by plastic deformation under high strain is approximately:

$$\Delta T = \frac{\beta \sigma \varepsilon}{\rho C_v} \quad (2)$$

where β is a constant representing the fraction of plastic deformation work converted to heat, usually taken to be 0.9; ρ is the density of the material, σ is the plastic flow stress, ε is the plastic strain, and C_v is the heat capacity at constant volume. For the present work, ρ is assumed to be 5.9 g/cm³, C_v is approximately 500 J/kg·K, σ ranges between approximately 4 and 6 GPa, $\varepsilon = \frac{4}{3} \ln \frac{\rho_1}{\rho_2}$ [28], ε is approximately 0.22 (with ρ_1 , or initial density, and ρ_2 , or shock density, respectively, being 4.13 and 4.88 g/cm³). Using equation (2), the maximum adiabatic temperature rise (ΔT) in the powder compacts is approximately 602 K, which is not sufficient to anneal the disorder in the shocked compacts.

4.2. Dynamic recovery and shear band formation

The adiabatic shear bands (ASBs) observed in mechanically alloyed NiAl particles and in the shock-consolidated bulk samples indicate the occurrence of dynamic recovery. ASBs [29] are formed during high strain deformation processes, and are typically observed during shock compaction, machining, grinding, forging, and even rolling. They are characterized in appearance by bands spanning across grain boundaries without preferred crystallographic orientation and are planar in form, with planes which are related to the specimen geometry and the deformation process rather than to the crystallography of the deforming material [30]. Insufficient time for the heat associated with the deformation to dissipate from the deformed area

causes the heat to soften this localized region. If the strength loss is greater than the strength gain due to deformation hardening, localized deformation will become unsteady, and deformation by ASBs can occur. ASBs are typically observed in a compressive stress state rather than in a state of tension.

The crystal structure of B2–NiAl (as shown in Fig. 13) should have 48 slip systems. However, NiAl is only reported to deform by {110}{001} slip [31]. The three independent slip systems are not enough to accommodate uniform plastic deformation by dislocation movements. In the case of high strain generated from ball milling and shock compaction, once crystallographic slip commences at a grain where the condition for slipping is satisfied, the slip will propagate into adjacent grains by cooperative slip or cross-slip, leading to the formation of shear localization across several grains. No evidence of twinning was observed in either the ball-milled or shock-compacted NiAl, which seems in agreement with the theory that shear bands for b.c.c. metals are associated with deformation by slip alone [30].

4.3. Strengthening mechanisms for shock-compacted NiAl intermetallic

In the present work, the hardness of NiAl was observed to increase with grain size refinement. The high hardness values obtained for shock-compacted mechanically alloyed nanostructured NiAl are attributed to the Hall–Petch strengthening effect [32]. The Hall–Petch strengthening mechanism is based on dislocation pile up at grain boundaries, or dislocation slip being impeded at grain boundaries. According to Jain and Christman [1], who studied the Fe–28Al–2Cr system, the grain boundary strengthening mechanism more appropriate for nanosized materials is the one developed by Li [33] based on dislocation generation from grain boundary ledges. According to this model, the macroscopic shear yield strength is expressed by the following equation:

$$\sigma = \sigma_0 + \alpha \mu b \left(\frac{8m}{\pi d} \right)^{\frac{1}{2}}$$

where σ_0 is the shear flow strength for coarse-grained material, α is a material constant, μ is the shear modulus, m is the ledge density, and d is grain size. The yield stress is still inversely proportional to the square root of grain size. However, dislocation pile ups and grain boundary stress concentrations are not required. It is believed the grain boundary dislocations form a Taylor dislocation forest, which inhibits dislocation motion and provide strengthening.

Hardness measurements as a function of grain size in the nanocrystalline NiAl compacts of the present work were combined with a series of hardness measurements obtained by other

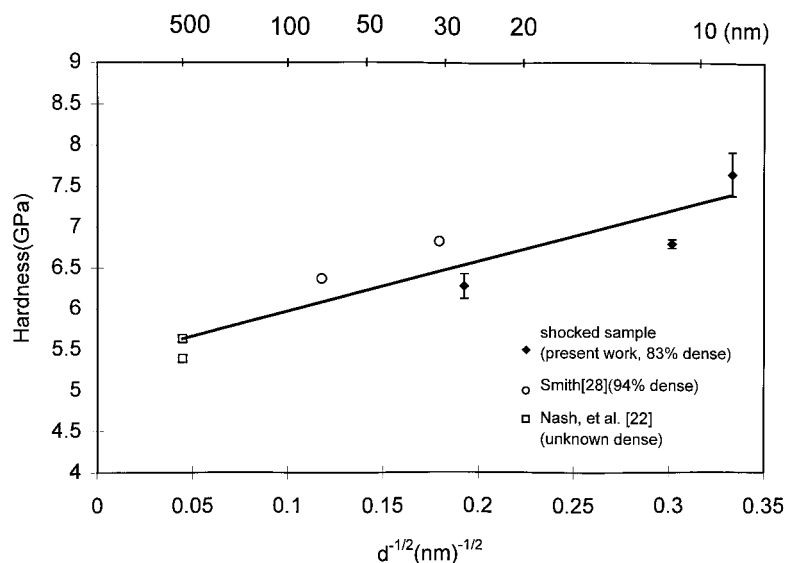


Fig. 14. Hall-Petch plot for NiAl based on present work on nanocrystalline NiAl compacts and data from Smith [32] and Nash *et al.* [22].

researchers [21, 22, 32]. As shown in the Hall-Petch plot in Fig. 14, a slope of approximately $6.14 \text{ GPa}(\text{nm})^{1/2}$ is indicated for the combined data. Considering α to be in the range of 0.2 to 0.4, b equal to 0.29, and μ approximately 77 GPa [36], Hall-Petch slope of $6.14 \text{ GPa}(\text{nm})^{1/2}$, results in mb equal to 0.1–0.2, consistent with the ledge mechanism model [29]. Further experiments are currently in progress, in which the grain size will be changed via heat treatment to obtain a much better correlation of hardness with grain size. The results of these experiments will be published at a later time. The Hall-Petch behavior for NiAl with grain sizes ranging from 13 μm to 70 μm at room temperature has been studied by Nagpal and Baker [34], who found it to be independent of grain size within this grain size range. However, Bowman *et al.* [35] have observed yield strength dependence on grain size over the 10 to 200 μm grain size range, a Hall-Petch slope of $0.522 \text{ MPa}(\text{m})^{1/2}$ [or $49.5 \text{ GPa}(\text{nm})^{1/2}$ for hardness]. Comparison of the Hall-Petch behavior in the nano- and micro-meter grain size range for Ni–Al indicates different slopes, but a similar strengthening mechanism.

The presence of Fe is also expected to contribute to the strengthening of NiAl, due to solution strengthening. In the present work iron was detected as a contaminant ($\approx 0.35\text{--}3.2 \text{ at.}\%$), a result of the abrasion of the steel balls and vial. The Fe content increases with increasing ball milling time. The effects of iron on the mechanical and physical properties of NiAl have been investigated by others [37–41]. According to Hosoda [37] and Fu *et al.* [38], ternary elements such as iron have site preference in aluminides because of their electronic structure. It is also reported that the site position of Fe additions in Ni-rich NiAl depends

on both temperature and on the amount of iron. In Al-rich (i.e. $x \geq 50$) alloys, the Fe atoms exist as substitutional antisite defects, i.e. the Fe atoms occupy Ni sublattices exclusively, which can hinder their detection during XRD and electron diffraction analysis. According to Lim *et al.* [39], the effect of iron doping is to stabilize the hardness of NiAl, and sometimes even increase the hardness at appropriate concentrations. Baker *et al.* [42] studied the lattice resistance (σ_0) and the Hall-Petch slope (κ) as a function of aluminum, and found that both σ_0 and κ are the smallest at the stoichiometric composition and increase with decreasing aluminum concentration. Hence, the contamination of iron is expected to contribute to the solute strengthening of NiAl.

5. CONCLUSIONS

Stoichiometric nanocrystalline B2-phase NiAl intermetallic was synthesized by 5 h or more of mechanical alloying via ball milling, using an elemental mixture of Ni and Al powders with a ball-to-powder weight ratio of approximately 3.

The nanostructured NiAl powders were consolidated into bulk compacts with a relative density of 83%, using shock compaction at a peak pressure of 4–6 GPa.

The microstructure of both mechanically alloyed particles and shock-densified compacts exhibits defects that include distorted regions, dislocations, grain boundaries, subgrains, and shear bands. The disordering induced in both mechanically alloyed and shock-compacted material ranges between 0.82 and 0.63.

Inhomogeneous deformation by shear bands appears to be the cause of dynamic recovery occur-

ring during ball milling and shock consolidation of NiAl, resulting in grain size refinement.

The Vickers hardness of NiAl increases with grain size refinement, and was found to be significantly greater than conventional NiAl intermetallic alloys. The Hall–Petch strengthening (dominated by dislocation ledge mechanism), as well as solute strengthening (due to Fe contamination), appear to contribute to the very high hardness of the nanocrystalline NiAl compacts.

Acknowledgements—This material is based upon work supported by the National Science Foundation under Grant No. DMR 9624927, and also by the U.S. Army Research Office, Grant No. DAAG55-97-1-0163. The authors gratefully acknowledge the assistance from K. Vandersall and R. Russell with the shock compaction experiments.

REFERENCES

- Jain, M. and Christman, T., *Acta mater.*, 1994, **42**, 1901.
- Siegel, R.W. and Fougere, G.E., *Mater. Res. Soc. Symp. Proc.*, 1995, **362**, 219.
- Chang, H., Hofler, J., Altstetter, C. and Averbach, R.S., *Mater. Sci. Engng*, 1992, **A153**, 676.
- Huang, B.-L. and Lavernia, E.J., *J. Mater. Syn. Proc.*, 1995, **3**, 1.
- Miracle, P.B., *Acta metall.*, 1993, **41**, 649.
- Davis, R.M., McDermott, B. and Koch, C.C., *Metall. Trans.*, 1988, **19A**, 2867.
- Fecht, H.J., Hellstern, E., Fu, Z. and Johnson, W.L., *Metall. Trans.*, 1990, **21A**, 2333.
- Smith, T.R., *Mater. Res. Soc. Symp. Proc.*, 1994, **350**, 219.
- Atzmon, M., *Phys. Rev. Lett.*, 1990, **64**, 487.
- Pyo, S.G., Kim, N.J. and Nash, P., *Mater. Sci. Engng*, 1994, **A181–A182**, 1169.
- Haff, G.R. and Schulson, E.M., *Metall. Trans.*, 1982, **13A**, 1563.
- Glade, S.C. and Thadhani, N.N., *Metall. Trans.*, 1995, **26A**, 2565.
- Gomdin, W.H., *Prog. Mater. Sci.*, 1986, **30**, 39–80.
- Thadhani, N.N. and Vreeland, T., *Acta mater.*, 1986, **34A**, 2323.
- Raybould, D., Morris, D.G. and Cooper, G.A., *J. Mater. Sci.*, 1979, **14**, 2523.
- Connihan, P., Nanostructured single-phase Ti₅Si₃ produced by crystallization of mechanically amorphized and shock-densified powder compact. M.S. thesis, Georgia Institute of Technology, Atlanta, GA, 1997.
- JCPDS Card Index Number 2-1261, JCPDS International Center for Diffraction Data, 1986.
- Huang, J.Y., Yu, Y.D., Wu, Y.K., Li, D.X. and Ye, H.Q., *Acta mater.*, 1997, **45**, 113.
- Cotrell, A.H., *Dislocations and Plastic flow in Crystals*. Clarendon Press, Oxford, 1972, p. 162.
- Haubold, T., Bohn, R., Birringer, R. and Gleiter, H., *Mater. Sci. Engng*, 1992, **A153**, 679.
- Christman, T. and Jain, M., *Scripta metall.*, 1991, **25**, 767.
- Nash, P., Ur, U.C. and Dollar, M., in *Proc. 2nd Int. Conf. Struct. Appl. Mech. Alloying*. Vancouver, Canada, 1993. ASM International, Materials Park, OH, p. 192.
- Bragg, W.L. and Williams, E.J., *Proc. R. Soc. A*, 1935, **151**, 540.
- Kubaschewski, O., *Trans. Faraday Soc.*, 1958, **54**, 814.
- Oelsen, W. and Middel, W., *Mitt. K. Wilhelm-Inst. Eisenforsch*, 1937, **19**, 1.
- Dannohl, H.D. and Lukas, H.L., *Z. Metallk.*, 1974, **65**, 642.
- Henig, E.T. and Lukas, H.L., *Z. Metallk.*, 1975, **66**, 98.
- Meyers, M.A., *Dynamic Behavior of Materials*. Wiley, New York, 1994, p. 388.
- Zener, C. and Hollomon, J.H., *J. appl. Phys.*, 1944, **15**, 22.
- Hatherly, M. and Malin, A.S., *Scripta metall.*, 1984, **18**, 449.
- Baker, I. and Schulso, E.M., *Metall. Trans.*, 1980, **15A**, 1129.
- Smith, T.R., *Mater. Res. Soc. Symp. Proc.*, 1995, **362**, 245.
- Li, J.C.M., *Trans. metall. Soc. A.I.M.E.*, 1963, **227**, 247.
- Nagpal, P. and Baker, I., *Scripta metall.*, 1990, **24**, 2381.
- Bowman, R.R., Noebe, R.D., Raj, S.V. and Locci, I.E., *Metall. Trans.*, 1992, **23A**, 1493.
- Viswanadham, R.K., Mannan, S.K., Kumar, K.S. and Wolfenden, A., *J. Mater. Sci. Lett.*, 1989, **8**, 409.
- Hosoda, H., Inoue, K. and Mishima, Y., *Mater. Res. Soc. Symp. Proc.*, 1995, **364**, 437.
- Fu, C.L. and Zou, J., *Mater. Res. Soc. Symp. Proc.*, 1995, **364**, 91.
- Lim, Y.J., Hong, K.T., Levit, V. and Kaufman, M.J., *Mater. Res. Soc. Symp. Proc.*, 1995, **364**, 273.
- Darolia, R., Lahrman, D.F. and Field, R.D., *Scripta metall.*, 1992, **26**, 1007.
- Liu, C.T., *Mater. Res. Soc. Symp. Proc.*, 1993, **288**, 3.
- Baker, I., Nagpal, P., Liu, F. and Munroe, P.R., *Acta mater.*, 1991, **39**, 1637.